https://doi.org/10.2352/ISSN.2470-1173.2019.12.HVEI-207

Investigation of the effect of pupil diameter on visual acuity using a neuro-physiological model of the human eye

Csilla Timár-Fülep, Gábor Erdei; Department of Atomic Physics, Budapest University of Technology and Economics; Budapest, Hungary

Abstract

Human visual acuity strongly depends on environmental conditions. One of the most important physical parameters affecting its value is the pupil diameter, which follows changes in the surrounding illumination by adaptation. Thus, the direct measurement of its influence on visual performance would require either medicaments or inconvenient apertures placed in front of the subjects' eyes to examine different pupil sizes, so it has not been studied in detail yet. In order to analyze this effect directly, without any external intervention, we accomplished simulations by our complex neuro-physiological vision model. It considers subjects as ideal observers limited by optical and neural filtering, as well as neural noise, and represents character recognition by template-matching. Using the model, we reconstructed the monocular visual acuity of real subjects with optical filtering calculated from the measured wavefront aberration of their eyes. According to our simulations, 1 mm alteration in the pupil diameter causes 0.05 logMAR change in the visual acuity value on average. Our result is in good agreement with former clinical experience derived indirectly from measurements that had independently analyzed the effect of background illumination on pupil size and on visual quality.

Introduction

As the most important factor to the patient, visual acuity is the primary outcome measure in ophthalmology. In clinical practice, relevant treatment effects are specified and justified in terms of 'change in visual acuity from baseline' [1], [2]. Most of the treatment criteria are based on the measured progression in visual acuity, using different expectations in letter scores (e.g. > 5 letters or > 10 letters). These criterions should be determined to be well distinguishable from the test-retest variability (*TRV*) of the measurements [3], [4].

Conventional acuity tests are performed by using eye charts. The subject's task is to correctly recognize characters, the size of which decreases from line to line. In order to enhance the reliability and repeatability of measurements, protocol standardization was required [2], which has been realized by the introduction of the Early Treatment Diabetic Retinopathy Study (ETDRS) chart [5], [6]. In this, the only significant variable that changes from one line to the other is the letter size, usually characterized by the α visual angle, describing the viewing angle of the stroke width of optotypes at the subject's eye. According to the logMAR notation (Minimum Angle of Resolution), the s letter size is expressed by the decimal-base logarithm of α given in minutes of arc:

$$s \equiv \log_{10}\alpha\,, \quad [\alpha] = \text{arcmin}. \tag{1}$$

The accuracy of the measurements, which limits the lower boundaries of observable progression, is affected by statistical and systematic errors. The former occurs during the evaluation of the trials due to uncertainties in the subject's visual system. According to the literature [1], [4], [6], using nonlinear regression to determine visual acuity results in the smallest available *TRV* (±0.04 logMAR) without causing any systematic error. In this case, the measured P recognition probability scores of the subject at the examined letter sizes are fitted by a monotonic differentiable S-shaped curve, the so-called psychometric function of vision [7], [8], [9]. Then, the V visual acuity value is specified by that particular s_0 letter size at which the $L(s)$ psychometric function intersects the standard $P_0 = 0.5$ probability threshold [5]:

$$L(s)\Big|_{s=s_0} = P_0 \Rightarrow V \equiv s_0\,, \; [V] = \text{logMAR}. \tag{2}$$

In addition to the above-mentioned statistical effects, the total error of the trials is also influenced by systematic errors. These are caused by the inappropriate adjustment, as well as temporal changes of the measurement parameters, and deteriorate the comparability of the results. Therefore, in order to provide sufficient precision for the investigation of disease progression and treatment efficacy, the effects of systematic error sources also have to be addressed [2], [6], [10]. The most important factors affecting visual acuity measurements are changes in the surrounding illumination of the room [11], [12], [14], or in the background illumination of the test chart [15], [16], and alteration of the viewing distance. The quantified effect of these error sources are listed in Table 1.

Table 1. Most important systematic error sources of visual acuity measurements.

Error type	Parameter change	ΔV [logMAR]
Surrounding illumination	100±15 cd/m^2	±0.05
Eye chart illumination	100…200 cd/m^2	±0.02
Viewing distance	4±0.5 m	±0.05

The illumination of the acuity chart and the viewing distance are standardized parameters [5]. Even though their specification may differ from country to country, the actual values in an examination room are always fixed, and completely independent of the tested subject. However, there is no such strict regulation on the surrounding illumination of the room, despite the fact that its variation modifies both the pupil size and the visual acuity value [12], [13], [14], [17]. Although standardization would enhance the comparability of the measurements, the remarkable variance of the pupil size of different subjects, even measured at identical illumination (±1.5 mm [17]), still distorts the results. Considering its importance, and since the influence of pupil size on visual acuity has been examined only indirectly by independent measurements [17], we decided to investigate the effect directly. Instead of

measurements, that would require medicaments to dilate /contract the pupil, or disturb the subjects by other means such as artificial apertures, we performed personalized acuity simulations by our calibrated neuro-physiological vision model [19]. By this tool, we can reconstruct the monocular visual acuity value of any subject based on the wavefront aberration and pupil diameter of his/her eye.

In this paper, first we give a brief description of the merits and innovation of our vision model, as well as the scoring and evaluation methods we developed to reduce uncertainty. Then, we present the results of our simulations to evince the influence of pupil size on visual acuity, and finally we compare the outcomes to former observations presented in the literature.

Methods

In order to examine the effect of pupil size on visual acuity in detail, we performed acuity simulations by our personalizable neuro-physiological vision model presented in [19]. It comprises of a physiological eye scheme supplemented by a neural model characterizing neural transfer, as well as additive noise, and cortical recognition. The schematic eye is implemented in Zemax Optic Studio [20], which allows for subject-specific customization, and ensures accurate description of the optical transfer by ray tracing and scalar diffraction analysis. The neural model is implemented in Matlab [21] to facilitate the numerical filtering steps of image processing and template-matching [22]. A brief summary of the model is presented below, while further details are explained in [19].

Neuro-physiological model of the human eye

Our physiologically accurate schematic eye is based on the widespread, historical Gullstrand Exact (number one) model [23], [24]. In order to include the severe longitudinal chromatic aberration of the human eye in our model [25], [26], we implemented chromatic dispersion by fitting the coefficients of the Sellmeier 1 formula to Atchison and Smith's measurements [27], instead of the original fixed refractive indices of the Gullstrand Exact scheme. Our model represents the Styles-Crawford effect (i.e. the directional sensitivity of the cones) as a Gaussian apodization factor in the amplitude transmission of the pupil according to [23].

The scheme can be personalized by monochromatic wavefront aberration (i.e. Optical Path Difference, *OPD*) usually measured by Shack-Hartmann sensor. The coefficients of the Zernike polynomial fitted to the wavefront of the subject [25], [28] can be directly input to the model. Accordingly, the first surface of the crystalline lens is modified to be a so-called Zernike-surface, the parameters of which should be optimized according to measurement results (providing an exact fit at the reference wavelength: $\lambda_0 = 555$ nm).

In order to take subject-specific adaptation to surrounding illumination into account, the d entrance pupil diameter must be adjusted to the particular value at which the visual acuity is to be determined. Then, the axial retina position is optimized for an object distance that corresponds to the refractive power of the subject's prescription glasses (the simulation assumes a relaxed eye gazing at infinity).

The polychromatic diffraction Point Spread Function (*PSF*) is determined by applying 24 equally distributed discrete wavelengths in the visible spectral range weighted according to the photopic sensitivity curve of the eye [17]. A representative wavefront, and the corresponding *PSF*, together with the eye scheme is depicted in Figure 1.

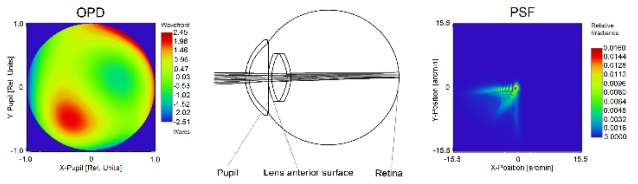

Figure 1. The measured wavefront aberration (OPD) of subject S. T.'s OD eye, and the corresponding polychromatic PSF at d = 5 mm entrance pupil diameter, together with the schematic view of the model eye.

The above-calculated *PSF* serves as the only input data of the neural model implemented in Matlab. Since visual systems are considered as linear, the subsequent steps of optical and neural image processing are described by spatial domain convolution at the retina [22], [29]. To enhance computational efficiency, we replaced convolutions with simple multiplications in the frequency domain [19]. First, we determine the inverse Fourier transform of the *PSF*, i.e. the Optical Transfer Function (*OTF*) [18], [30], and calculate the subject-specific optically filtered retinal image. Then, we apply low-level retinal and neural image processing: edge-enhancement, which is characterized by the average Neural Transfer Function (*NTF*) derived from contrast sensitivity and optical transfer measurements presented in the literature [18], [31], [32], [33].

After optical and neural filtering, the effect of neural noise is taken into account. Our model represents neural noise so that it corresponds to the individual cells of the retinal cone lattice (i.e. a hexagonal structure with 120 cycles/degree sampling frequency) [26], [29], [33]. It is implemented as additive Gaussian white noise, the σ^2 variance of which is a free parameter of the model, differentiating between subjects' neural sensitivity. We calibrated its average value by measurements: $\sigma_{ave} = 0.10$ [19]. The end-result of the subsequent steps of image processing, i.e. the noisy neural representation, is illustrated in Figure 2.

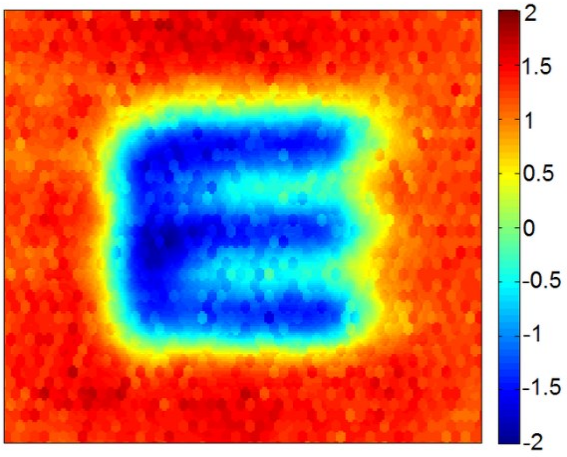

Figure 2. The end-result of optical and neural image processing performed by our model: noisy neural representation of an image of letter "E".

Our vision model considers subjects as ideal observers (like those, who are not supposed to tell intentionally wrong guesses to trials) limited by optical and neural filtering, as well as neural noise. It realizes character recognition by a template-matching algorithm [32], [34], which quantifies the similarity between the currently examined object and several templates stored in the brain.

According to the literature [31], [32], [34], in our model the template set contains optically and neurally filtered, but *noiseless* images of all 26 letters of the English Alphabet calculated for each letter size in case of a given subject.

The implemented recognition method determines the ρ correlation value of the examined image and a template as the maximum element of the Pearson's cross-correlation matrix, which ensures translation invariance for recognition [35]. When testing a given character, the correlation values for all possible templates are calculated, and then sorted in descending order to find the maximum: ρ_{max}. Our model imitates the decision-making method of subjects, who often become hesitating during visual acuity tests near the recognition threshold, and cannot decide between multiple options [9], [10]. This tendency suggests that differences below a certain level cannot be distinguished, thus we defined a $\delta\rho$ discrimination range in which the identification of any differences is not possible. In our vision model, "indistinguishability" is bound to an absolute limit, and $\delta\rho$ is determined as a constant value, being the second free parameter. Its calibrated average value equals $\delta\rho_{ave} = 0.0025$.

In agreement with the above-discussed considerations, the character recognition process determines a set of potential answers for one given tested letter corresponding to the correlation values within the $[\rho_{max}-\delta\rho; \rho_{max}]$ discrimination range. Then, each potential answer is assessed by a special correlation-based scoring scheme, which quantifies the similarity of the examined-identified letter pairs by "Optotype Correlation" (*OC*) [36], [37]. The *OC* values of the character pairs are determined by the same cross-correlation algorithm as used for template-matching, but in this case based on the non-distorted ideal images of the letters. Thus, the output of our model for the tested letter is the mean *OC* value corresponding to the potential answers.

Visibility of a set of letters at the same size can be characterized by "Rate of Recognition" (*RR*), i.e. the average *OC* value of the tested letters [36], [37]. *RR* is directly comparable to the *P* recognition probability, but provides more information about the quality of vision [36], [37]. Using the *RR* values calculated at all letter sizes, our model determines visual acuity by nonlinear regression such as:

$$L(s)\Big|_{s=s_0} = RR_0 \Rightarrow V \equiv s_0 \,. \tag{3}$$

Based on our preliminary measurements, in case of *RR* the threshold corresponding to the $P_0 = 0.5$ definition without any bias is $RR_0 = 0.68$ [36]. We describe the profile of the *L(s)* psychometric function by a linearly transformed logistic function with asymptotes adjusted to the theoretical *RR* values according to the total number of possible answers (i.e. all 26 letters of the English Alphabet) [7], [8], [9]:

$$L(s) = \frac{25}{26} \cdot \frac{1}{1+\exp\left(-4k(s-s_{mp})\right)} + \frac{1}{26} \tag{4}$$

Its two parameters, s_{mp} and k, are determined by nonlinear regression by fitting (4) to the calculated (s, *RR*) points of a given subject. The result of a representative visual acuity simulation (subject S. T.'s OD eye) is demonstrated in Figure 3.

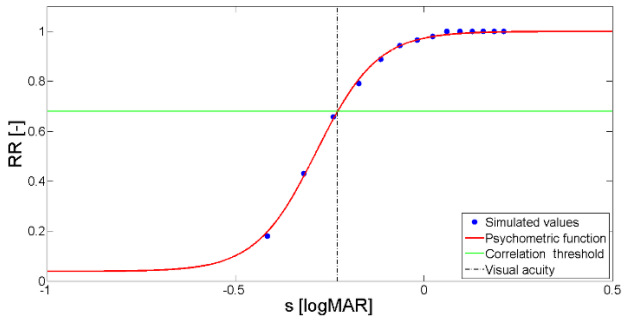

Figure 3. The output of a representative simulation (subject S. T.'s OD eye): the calculated RR values, the fitted psychometric function, the correlation threshold, and the resulting visual acuity value.

Based on our former calibration measurements and simulations [19], the residual error equals 0.045 logMAR, which gives a rough estimate of the accuracy available by our simulation. As a comparison: the accuracy of standard ETDRS trials is 0.06,…,0.15 logMAR [1], [3], [4].

Subject pool, auxiliary measurements

The vision model was used to simulate the acuity of 10 healthy young subjects whose visual acuity was between 0,…,−0.4 logMAR, within the calibration range of the model [19], and close to the range of normal vision: −0.1,…,−0.2 logMAR [17], [1]. Wavefront aberration of the subjects' eyes was measured by a clinical Shack-Hartmann sensor (WASCA Asclepion Zeiss Wavefront Analyzer, Sw 1.41.6; Carl Zeiss Meditec AG, Germany), and used to personalize the simulation through the eye scheme.

Determination of the effect of pupil size

We examined the effect of pupil size through simulations performed by our vision model, in which any particular entrance pupil diameter can be set as a simple input parameter. We accomplished multiple simulations with different pupil sizes, and determined the acuity value for each case separately. Our purpose was to analyze a wide pupil size range relevant for ophthalmologists, thus we swept the diameter from 2 to 6 mm with 1 mm increment. In order to investigate subject-specific effects, we personalized the simulations by measured wavefront aberration. Although we gathered all data for the subjects' both eyes, we considered only their right eyes (OD) in our analysis, because the two eyes of a person are often strongly correlated [39].

Results

In order to directly demonstrate the significant effect of pupil size on visual acuity [13], [17], [18], we analyzed the alteration of the psychometric function with respect to pupil diameter. To present subject-specific outcomes in detail, we examined the shape of the psychometric curve described by Eq. (4). A representative result consisting the psychometric functions of subject S. T.'s OD eye corresponding to all examined pupil sizes is illustrated in Figure 4.

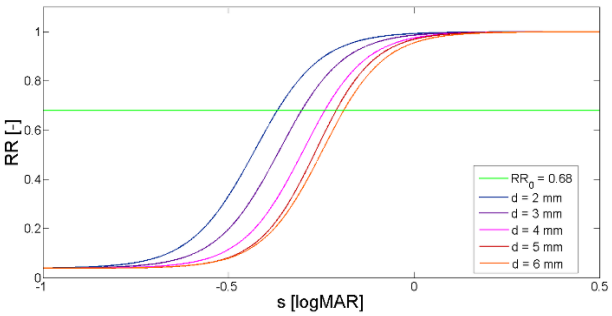

Figure 4. The effect of pupil size on the psychometric function of vision based on simulations performed by the personalized model of subject S. T.'s OD eye with different pupil diameters.

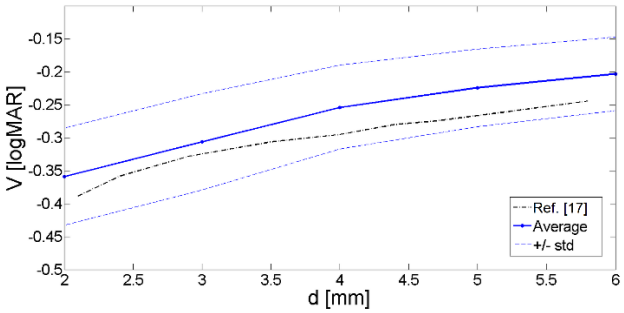

Figure 5. The average change of the visual acuity value with respect to pupil size in the 2,…,6 mm diameter range. The black dash-dot line represents the average curve corresponding to standard 90 cd/m^2 chart illumination presented in [17].

The figure clearly shows the significant impact of the pupil size. However, in order to present quantitative results besides the illustration, we determined V according to Eq. (3), which is the eventual outcome of the simulation. The acuity values derived from the performed analyses are presented in Table 2.

Table 2. Results of individual acuity simulations performed with different pupil diameters in the 2,…,6 mm range relevant for ophthalmologists.

Subject \ pupil diameter	*V* [logMAR]				
	2 mm	3 mm	4 mm	5 mm	6 mm
Ku. Ma.	-0.43	-0.41	-0.35	-0.31	-0.29
G. A.	-0.36	-0.31	-0.22	-0.21	-0.18
M. T.	-0.35	-0.26	-0.24	-0.22	-0.19
P. B.	-0.31	-0.29	-0.23	-0.18	-0.17
S. T.	-0.37	-0.30	-0.24	-0.21	-0.19
U. F.	-0.41	-0.36	-0.29	-0.27	-0.25
R. I.	-0.41	-0.34	-0.29	-0.26	-0.25
Kl. Mi.	-0.17	-0.13	-0.10	-0.09	-0.07
S. O.	-0.38	-0.31	-0.27	-0.25	-0.22
G. T.	-0.40	-0.34	-0.27	-0.24	-0.21

Based on these results, one can see that 1 mm alteration in the pupil diameter can cause 0.02,…,0.07 logMAR change in the visual acuity value. The effect is more significant in case of smaller pupil sizes, which is in good agreement with the fact that pupil contraction cuts off the edge of higher order aberrations. Further comprehensive analysis of the simulation results is presented in the next section.

Discussion

In order to formulate a more general statement for subjects with normal and supernormal vision, we made statistics on the individual results of the examined subject group. We determined the average visual acuity value and its standard deviation over the subjects for each tested pupil size. According to the results, 1 mm modification of the pupil size causes 0.05 logMAR (i.e. half a line) change in the acuity value on average. The dependence of the average visual acuity as a function of pupil diameter is depicted in Figure 5.

In order to confirm the validity of our simulations, we compared our results to the observations presented in the literature [17]. Since the direct influence of pupil diameter on visual acuity has not been studied yet, we estimated it through its relation with background illumination [11], [13], [14]. Despite the result is a combination of independent measurements performed under different conditions with different subjects, the outcome is in good agreement with our direct simulations (see black dash-dot line in Figure 5).

Conclusions

In order to determine the direct influence of pupil size on visual acuity, we performed personalized acuity simulations by our neuro-physiological vision model. It reconstructs the monocular visual acuity value of real subjects based on the wavefront aberration and the pupil diameter of their eye. According to our results, 1 mm alteration of the entrance pupil diameter causes 0.05 logMAR change in the acuity value on average. Our results are well supported by clinical experience derived indirectly from measurements presented in the literature. Due to its significant influence compared to other environmental conditions, we suggest that it would be fairly important to keep the surrounding illumination of the examination room at a standard level. Furthermore, in order to take subject-specific pupil adaptation into account, the entrance pupil diameter should be recorded besides the measured visual acuity value as well. Our experience shows that a simple camera system with ±0.5 mm spatial accuracy is feasible without high financial resources, and the obtained pupil diameter values would provide a great contribution to the comparability and consistency of visual acuity measurements.

Acknowledgement

The authors are extremely grateful to the colleagues of the Department of Atomic Physics, Budapest University of Technology and Economics, and Medicontur Medical Engineering Ltd. who took their time from their busy schedules to participate in the measurements. As well as, we would like to thank Dr. Illés Kovács and Dr. Kinga Kránitz for their valuable contribution in wavefront aberration measurements.

The research has been supported by the Ministry of National Development (NFM) in a competitiveness and excellence contract for the project "Medical technological research and development on the efficient cure of cataract" VKSZ-12-1-2013-80.

Supported by the ÚNKP-18-3 New National Excellence Program of the Ministry of Human Capacities.

References

[1] M. E. Vanden Bosch, and M. Wall, "Visual acuity scored by the letter-by-letter or probit methods has lower retest variability than line assignment method," Eye (London, England), vol. 11, pp. 411-417, 1997.

[2] N. Shah, S. C. Dakin, H. L. Whitaker, and R. S. Anderson, "Effect of scoring and termination rules on test–retest variability of a novel high-pass letter acuity chart," Investigative Ophthalmology and Visual Science, vol. 55, no. 3, pp. 1386-1392, 2014.

[3] J. Siderov, and A. L. Tiu, "Variability of measurements of visual acuity in a large eye clinic," Acta Ophthalmologica Scandinavica, vol. 77, no. 6, pp. 673-676, 1999.

[4] A. Arditi, and R. Cagenello, "On the statistical reliability of letter-chart visual acuity measurements," Investigative Ophthalmology & Visual Science, vol. 34, no. 1, pp. 120-129, 1993.

[5] International Council of Ophthalmology, Visual Functions Committee, "Visual acuity measurement standard, ICO 1984," Italian Journal of Ophthalmology, II/I, pp. 1-15, 1988.

[6] C. A. Hazel, and D. B. Elliott, "The dependency of logMAR visual acuity measurements on chart design and scoring rule," Optometry and Vision Science, vol. 79, no. 12, pp. 788-792, 2002.

[7] T. T. Norton, D. A. Corliss, and J. E. Bailey, The Psychophysical Measurement of Visual Function Ridgevue Publishing, 2014.

[8] F. A. Wichmann, and N. J. Hill, "The psychometric function: I. Fitting, sampling, and goodness of fit," Perception and Psychophysics, vol. 63, no. 8, pp. 1293-1313, 2001.

[9] A. Carkeet, "Modeling logMAR visual acuity scores: effects of termination rules and alternative forced-choice options," Optometry and Vision Science, vol. 78, no. 7, pp. 529-538, 2001.

[10] I. L. Bailey, and J. E. Lovie-Kitchin, "Visual acuity testing. From the laboratory to the clinic", Vision Research, vol. 90, pp. 2-9, 2013.

[11] S. Shlaer, "The relation between visual acuity and illumination," Journal of General Physiology, vol. 21, no. 2, pp. 165-188, 1937.

[12] R. J. Lin, J. S. Ng, and A. L. Nguyen, "Determinants and standardization of mesopic visual acuity," Optometry and Vision Science, vol. 92, pp. 559-565, 2015.

[13] F. W. Campbell, and A. H. Gregory, "Effect of Size of Pupil on Visual Acuity," Nature, vol. 187, no. 4743, pp. 1121-1123, 1960.

[14] C. A. P. Foxell, and W. R. Stevens, "Measurements of visual acuity," British Journal of Ophthalmology, vol. 39, pp. 513-533, 1955.

[15] J. E. Sheedy, I. L. Bailey, and T. W. Raasch, "Visual acuity and chart luminance," American Journal of Optometry and Physiological Optics, vol. 61, pp. 595-600, 1984.

[16] R. J. Lythgoe, The Measurement of Visual Acuity, Medical Research Council, Special Reports Series, H. M. Stationary, 1932.

[17] R. B. Rabbetts, Bennett and Rabbetts' Clinical Visual Optics, Butterworth-Heinemann, Elsevier, 2007.

[18] A. B. Watson, "A formula for the mean human optical modulation transfer function as a function of pupil size," Journal of Vision, vol. 13, no. 6, pp. 1-11, 2013.

[19] C. Fülep, I. Kovács, K. Kránitz, and G. Erdei, "Simulation of visual acuity by personalizable neuro-physiological model of the human eye," submitted to Scientific Reports, 2018.

[20] Zemax (Radiant Zemax, Redmond,WA), www.zemax.com

[21] The MathWorks Inc., "MATLAB: the language of technical computing," www.mathworks.com/products/matlab

[22] L. N. Teow, and K. F. Loe, "Robust vision-based features and classification schemes for off-line handwritten digit recognition," Pattern Recognition, vol. 35, no. 11, pp. 2355-2364, 2002.

[23] P. G. Gobbi, Modeling the Optical and Visual Performance of the Human Eye, SPIE Press, Bellingham WA, USA, 2013.

[24] D. A. Atchison and G. Smith, Optics of the human eye, Butterworth-Heinemann, Elsevier, 2000.

[25] L. N. Thibos, X. Hong, A. Bradley, and X. Cheng, "Statistical variation of aberration structure and image quality in a normal population of healthy eyes," Journal of the Optical Society of America A, vol. 19, no. 12, pp. 2329-2348, 2002.

[26] E. Dalimier, E. Pailos, R. Rivera, and R. Navarro, "Experimental validation of a Bayesian model of visual acuity," Journal of Vision, vol. 9, no. 7, pp. 1-16, 2009.

[27] D. A. Atchison, and G. Smith, "Chromatic dispersions of the ocular media of human eyes," Journal of the Optical Society of America A, vol. 22, no. 1, pp. 29-37, 2005.

[28] J. Liang, B. Grimm, S. Goelz, and J. F. Bille, "Objective measurement of wave aberrations of the human eye with the use of a Hartmann-Shack wave-front sensor," Journal of the Optical Society of America A, vol. 11, no. 7, pp. 1949-1957, 1994.

[29] A. G. Anderson, B. A. Olshausen, K. Ratnam, and A. Roorda, "A neural model of high-acuity vision in the presence of fixational eye movements," in 50th Asilomar Conference on Signals, Systems and Computers, Pacific Grove, CA, USA, 2016.

[30] J. D. Marsack, L. N. Thibos, and R. A. Applegate, "Metrics of optical quality derived from wave aberrations predict visual performance," Journal of Vision, vol. 4, no. 4, pp. 322-328, 2004.

[31] A. Faylienejad, "A computational model for predicting visual acuity from wavefront aberration measurements," M.Sc. thesis in Vision Science, University of Waterloo, 2009.

[32] A. B. Watson, and A. J. Ahumada, Jr., "Predicting visual acuity from wavefront aberrations," Journal of Vision, vol. 8(4), no. 17, pp. 1-19, 2008.

[33] P. G. J. Barten, Contrast Sensitivity of the Human Eye and its Effects on Image Quality, SPIE Optical Engineering Press, 1999.

[34] S. Schuster, and S. Amtsfeld, "Template-matching describes visual pattern-recognition tasks in the weakly electric fish Gnathonemus petersii," Journal of Experimental Biology, vol. 205, pp. 549-557, 2002.

[35] N. M. Oliver, B. Rosario, and A. P. Pentland, "A Bayesian computer vision system for modeling human interactions," IEEE Transactions on Pattern Analysis and Machine Intelligence, vol. 22, no. 8, pp. 831-843, 2000.

[36] C. Fülep, I. Kovács, K. Kránitz, and G. Erdei, "Correlation-based evaluation of visual performance to reduce the statistical error of visual acuity," Journal of the Optical Society of America A, vol. 34, no. 7, pp. 1255-1264, 2017.

[37] G. Erdei, and C. Fülep, "Measuring visual acuity of a client," Word Intellectual Property Organization, WO/2018/020281 A1, Appl. No. PCT/HU2016/000050, 2018.

[38] D. B. Elliott, K. C. H. Yang, and D. Whitaker, "Visual Acuity Changes Throughout Adulthood in Normal, Healthy Eyes: Seeing Beyond 6/6," Optometry and Vision Science, vol. 72, no. 3, pp. 186-191, 1995.

[39] R. J. Glynn, and B. Rosner, "Regression methods when the eye is the unit of analysis," Ophthalmic Epidemiology, vol. 19, no. 3, pp. 159-165, 2012.

Author Biography

Csilla Tímár-Fülep is a physicist PhD candidate at the Department of Atomic Physics, Budapest University of Technology and Economics. She received her BSc in physics (2013) and her MSc in medical physics (2015) from the same university. Her research focuses on the theoretical and experimental investigation, and numerical modeling of human visual acuity. She works in collaboration with ophthalmologists and industrial partners to develop intraocular lenses, which provide more comfortable visual experience than currently available products.

JOIN US AT THE NEXT EI!

IS&T International Symposium on

Electronic Imaging

SCIENCE AND TECHNOLOGY

Imaging across applications . . . Where industry and academia meet!

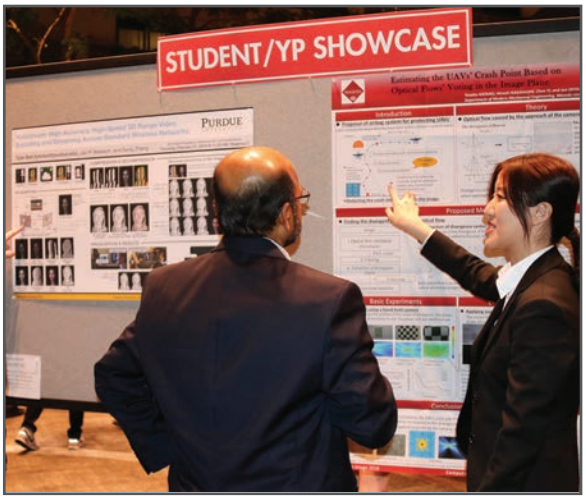

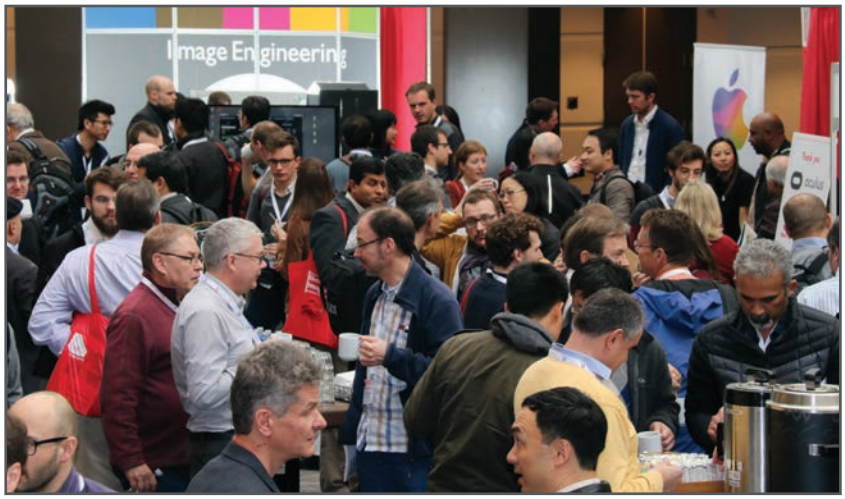

• SHORT COURSES • EXHIBITS • DEMONSTRATION SESSION • PLENARY TALKS •
• INTERACTIVE PAPER SESSION • SPECIAL EVENTS • TECHNICAL SESSIONS •

www.electronicimaging.org

IS&T
imaging.org